Author's Accepted Manuscript

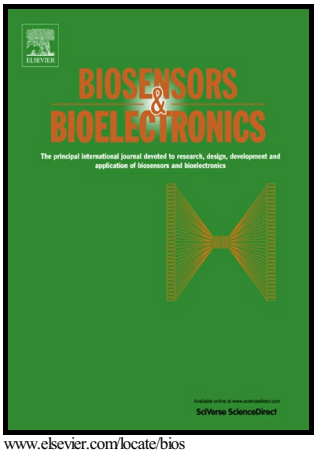


www.elsevier.com/locate/bios

# Nano-biosensor for highly sensitive detection of HER2 positive breast cancer

Razieh Salahandish, Ali Ghaffarinejad, Seyed Morteza Naghib, Keivan Majidzadeh-A, Hossein Zargartalebi, Amir Sanati-Nezhad

PII: S0956-5663(18)30398-1
DOI: https://doi.org/10.1016/j.bios.2018.05.043
Reference: BIOS10501

To appear in: *Biosensors and Bioelectronic*

Received date: 6 December 2017
Revised date: 10 May 2018
Accepted date: 24 May 2018

Cite this article as: Razieh Salahandish, Ali Ghaffarinejad, Seyed Morteza Naghib, Keivan Majidzadeh-A, Hossein Zargartalebi and Amir Sanati-Nezhad, Nano-biosensor for highly sensitive detection of HER2 positive breast cancer, *Biosensors and Bioelectronic,* https://doi.org/10.1016/j.bios.2018.05.043

This is a PDF file of an unedited manuscript that has been accepted for publication. As a service to our customers we are providing this early version of the manuscript. The manuscript will undergo copyediting, typesetting, and review of the resulting galley proof before it is published in its final citable form. Please note that during the production process errors may be discovered which could affect the content, and all legal disclaimers that apply to the journal pertain.

ACCEPTED MANUSCRIPT

# Nano-biosensor for highly sensitive detection of HER2 positive breast cancer

Razieh Salahandish[a,b,e,f], Ali Ghaffarinejad[a,b]*, Seyed Morteza Naghib[c], Keivan Majidzadeh-A[d]*, Hossein Zargartalebi[e,f], Amir Sanati-Nezhad[e,f]*

[a] Research Laboratory of Real Samples Analysis, Faculty of Chemistry, Iran University of Science and Technology (IUST), Tehran 1684613114, Iran

[b] Electroanalytical Chemistry Research Center, Iran University of Science and Technology (IUST), Tehran 1684613114, Iran

[c] Nanobioengineering Division, Department of Nanothechnology, School of New Technologies, Iran University of Science and Technology (IUST), Tehran 1684613114, Iran

[d] Genetics Department, Breast Cancer Research Center (BCRC), Motamed Cancer Institute, ACECR, Tehran, Iran

[e] BioMEMS and Bioinspired Microfluidic Laboratory, Department of Mechanical and Manufacturing Engineering, University of Calgary, Calgary T2N 1N4, Alberta, Canada

[f] Center for BioEngineering Research and Education, University of Calgary, Calgary T2N 1N4, Alberta, Canada

Accepted manuscript

E-Mail: ghaffarinejad@iust.ac.ir

E-Mail: kmajidzadeh@razi.tums.ac.ir

E-Mail: amir.sanatinezhad@ucalgary.ca

*Corresponding Authors

ACCEPTED MANUSCRIPT

**SI**: Supporting Information

Accepted manuscript

ACCEPTED MANUSCRIPT

Accepted manuscript

**ABSTRACT**:

Nanocomposite materials have provided a wide range of conductivity, sensitivity, selectivity and linear response for electrochemical biosensors. However, the detection of rare cells at single cell level requires a new class of nanocomposite-coated electrodes with exceptional sensitivity and specificity. We recently developed a construct of gold nanoparticle-grafted functionalized graphene and nanostructured polyaniline (PANI) for high-performance biosensing within a very wide linear response and selective performance. Further, replacing the expensive gold nanoparticles with low-cost silver nanoparticles as well as optimizing the nanocomposite synthesis and functionalization protocols on the electrode surface in this work enabled us to develop ultrasensitive nanocomposites

ACCEPTED MANUSCRIPT

for label-free detection of breast cancer cells. The sensor presented a fast response time of 30 min within a dynamic range of 10 – $5\times10^6$ cells.mL$^{-1}$ and with a detection limit of 2 cells.mL$^{-1}$ for the detection of SK-BR3 breast cancer cell. The nano-biosensor, for the first time, demonstrated a high efficiency of > 90% for the label-free detection of cancer cells in whole blood sample without any need for sample preparation and cell staining. The results demonstrated that the optimized nanocomposite developed in this work is a promising nanomaterial for electrochemical biosensing and with the potential applications in electro-catalysis and super-capacitances.

**KEYWORDS:** Single cell detection; Electrochemical biosensing; Nanostructured polyaniline nanocomposite; Breast cancer

Accepted manuscript

## 1- INTRODUCTION

Based on the World Health Cancer Organization, breast cancer, as the most frequent cancer among women, impacting over 1.5 million women each year, and causes the most significant cancer-related deaths among women. In 2015, 570,000 women died from breast cancer. In US alone, one in eight U.S. women (about 12%) develops invasive breast cancer during their lifetime (Winham et al. 2017) and about 45,000 women are expected to die in 2018 from breast cancer, although the mortality rate has been decreasing over last 10 years. Currently, the detection of breast cancer is routinely done by mammogram, which has significantly improved breast cancer outcomes, although it may not be able to distinguish between benign and malignant lesions (Hathaway et al. 2011).

ACCEPTED MANUSCRIPT

Also, invasive biopsy is needed to either confirm or rule out cancer. Mammography fails to detect 10-25% of breast cancers. Improvements in breast cancer detection would provide a tremendous benefit to cancer patients. Also, the ideal technology is expected to be inexpensive, rapid and with little or no discomfort to patients. Furthermore, reducing the false positive rate, even by a modest 10% while improving the sensitivity, may lead to improved screening and is a desirable goal.

One non-invasive method for cancer detection is to detect cells in the blood based on their surface biomarker proteins (Kearney and Murray 2009). Protein biomarkers have been extensively used for monitoring aggressive types of breast cancers (Ali et al. 2016). One specific biomarker over-expressed in 20–30% of human breast cancers is the human epidermal growth factor receptor 2 (HER2), named as $HER2^+$ (Cho et al. 2003; Gullick 2001; Slamon et al. 1987). The monitoring of HER2 cells is very beneficial as it is associated with very aggressive types of breast cancer tumors (Riccio et al. 2009). HER2 extracellular domain (ECD) can be detected in approximately 45% of patients with HER2-related breast cancers (Chan et al. 1994). An accurate assessment of HER2 positive cells is essential to identify patients who may benefit from drugs like herceptin or trastuzumab (Mass et al. 2005; Riccio et al. 2009).

The most common clinical testing procedures for detecting HER2 positive cancer cells involve taking a biopsy of the tumor and detecting these cancer cells using routine immunohistochemistry (IHC) assays, and gold standard fluorescence signals by in-situ hybridization (FISH) (Mass et al. 2005) and chromogenic in-situ hybridization (CISH) (Jiang et al. 2014).

These methods, however, are limited in one or several factors, including very invasive biopsies, costly labeling detection, long turn-around times, limited analytical sensitivity and target specificity, and lack of capacity to multiplexing (Gown 2008; Sieben et al. 2007). Several other methods have been developed for detecting $HER2^+$ circulating tumor cells (CTCs), including genomic and optical assays (Lu et al. 2010), fluorescence and scattering assays (Li et al. 2011; Tsai

Accepted manuscript

ACCEPTED MANUSCRIPT

et al. 2009), direct cell imaging (Galletti et al. 2014; Gao et al. 2011), and optical-based methods that detect cancer cells isolated within microfluidics by immunocapturing or filter techniques (Mayer et al. 2011; Reátegui et al. 2015). Filter-based techniques always and most of molecular techniques still require cell staining to count the number of cells and determine the type of the captured cells which requires microscopy and also limits the retrieval of live cells captured on the filter for further downstream molecular analysis (Khoo et al. 2018).

Rapid and label-free HER2 detection have been established using surface plasmon resonance (SPR) based method, piezoelectric micro-cantilever sensor (PEMSs), label-free capacitive aptasensor, opto-fluidic ring resonator (OFRR), ring resonator sensor, and surface acoustic wave (SAW) biosensors (Capobianco et al. 2008; Wang et al. 2009; Washburn et al. 2009; White et al. 2006). However, these techniques are limited in one or several factors such as high cost and long testing time due to the sandwich type design (Chung et al. 2006; Vaisocherová et al. 2009), and limited performance in HER2 detection in the human blood (Capobianco et al. 2008; Gruhl et al. 2010). Eelectrochemical sensing methods are usually preferred to other techniques due to the advantages of being portable, simple, easy to use, cost-eff ective, disposable, label-free, and lab-on-a-chip diagnostics (Han et al. 2018a; Han et al. 2018b; Wang et al. 2017). The “affibody” method was developed for selective detection of HER2 (Myung et al. 2011) as a rapid and selective diagnosis to use a nanoprobe for detection of HER2-expressing tumor and cell imaging (Gao et al. 2011).

Recently, we developed a nanocomposite based-gold nanoparticles for biosensing applications and applied it for the detection of ascorbic acid biomolecules (Salahandish et al. 2018). Further, replacement of expensive gold nanoparticles with low-cost silver nanoparticles as well as the optimization of the nanocomposite synthesis and functionalization protocols in the present work opened up the avenue for making ultrasensitive nanocomposites for label-free, rapid and low-cost

Accepted manuscript

ACCEPTED MANUSCRIPT

detection of cancer cells. In this work, we use a novel, highly sensitive and label-free strategy for electrochemical detection of HER2 as a breast cancer biomarker in human serum samples. Label-free biosensors usually have lower sensitivity than the labeled type due to the lack of auxiliary species (Ohno et al. 2010). However, our nano-biosensor achieved the detection limit of 2 cells.mL$^{-1}$ within a dynamic range of 10 – $5\times10^6$ cells.mL$^{-1}$. The biosensor performance relies on a significant signal enhancement by a graphene nanostructured PANI and silver nanoparticles (AgNPs). The sandwich model of functionalized nitrogen-doped graphene (NFG)/AgNPs/PANI multilayer structure, with a correct combination and arrangement of nanocomposite components, exhibited excellent conductivity and stability, and allowed more HER2 antigens of cancer cells to anchor to the electrode. Notably, this strategy eliminated the need for any biological enzymes, making the system simpler and universal.

## 2- EXPERIMENTAL

### *2-1 Materials and methods*

For synthesis of the nanocomposite, graphite fine powder (spectroscopic grade, particle size ≤ 50 µm), sodium nitrate ($NaNO_3$), sulfuric acid ($H_2SO_4$), potassium permanganate ($KMnO_4$), silver nitrate ($AgNO_3$), potassium nitrate ($KNO_3$) and aniline (99%) were purchased from Merch. 1-Ethyl-3-(3 dimethylaminopropyl) carbodiimide hydrochloride (EDC), N-hydroxysuccinimide (NHS), and dimethylformamide (DMF) were purchased from Sigma-Aldrich. For biosensing, potassium ferricyanide ($K_3Fe(CN)_6$) and potassium ferrocyanide ($K_4Fe(CN)_6$) were purchased from Merck. Phosphate-buffered saline (PBS), bovine serum albumin (BSA), Tween-20, fetal bovine serum (FBS) and monoclonal anti-HER2 antibody (AHAb) from human were purchased from Sigma-Aldrich. SK-BR3, ZR-75-1, MCF10, SW742, and MDA-MB231 cell lines were obtained from ATCC sources.

Accepted manuscript

ACCEPTED MANUSCRIPT

The field emission scanning electron microscope (FESEM) images were taken by Carl Zeiss FESEM instrument, model Sigma. The cancer cells captured on the electrodes were imaged and counted by Nikon ECLIPSE Ti microscope. All electrochemical stimulation and characterization were performed using a Potentiostat/Galvanostat, the model of Autolab PGSTAT 30 (Echo chemie, B. V.) and Nova 1.11 software. The electrochemical impedance spectroscopy (EIS) measurement was accomplished within the frequency range of $10^{-1}$ – $10^{5}$ Hz, with the potential amplitude of 14 mV around the open circuit potential ($E_{ocp}$).

*2-2 Synthesis of nanocomposite*

The nanocomposite developed in this study involved three layers and was deposited on the fluorine doped tin oxide (FTO) glass plates (8 Ω resistance) with a surface area of 0.25 $cm^2$. The first layer was the graphene layer and synthesized in two steps. In the first step, graphene oxide was synthesized using the modified Hammer method (Li et al. 2013) and functionalized with 100 μM NHS/400 μM EDC. In the second step, the NFG was reduced by DMF at its boiling point and then cast coated on the electrode surface (Cernat et al. 2015). The second layer was the AgNPs layer and electrodeposited on the first layer to increase the surface area and enhance the conductance charge transfer by dual potential chronoamperometry ($E_1$ and $t_1$; -0.4 V, 1 and 10 s; $E_2$ and $t_2$; 0.34 V, 30 and 90 s, respectively) in a solution containing 0.1 M $KNO_3$ and 1 mM $AgNO_3$ (Geboesa et al. 2014; Ustarroz et al. 2010). The PANI layer as the third layer was electropolymerized in 0.03 M aniline monomer and 0.5 M $H_2SO_4$ using cyclic voltammetry (CV) technique (20 cycles, scan rate 30 $mV.s^{-1}$, and in the range of -0.4 to 1.2 V) (Darowicki and Kawula 2004). All electrochemical tests were performed over the conventional three-electrode configuration consisting of Ag|AgCl|3 M $KNO_3$ reference electrode, Pt rod counter electrode, and modified FTO working electrode.

*2-3 Fabrication of the nano-coated biosensor*



Accepted manuscript

ACCEPTED MANUSCRIPT

Following the deposition of the three-layer nanocomposite construct on the electrode, the nanocomposite-prepared electrode was suspended in EDC (400 μM) and NHS (100 μM) (prepared with DI water) solution for 4 h at room temperature to functionalize the nanocoated construct with ―COOH group, followed by rinsing with PBS (0.02 M, pH = 7.4) (Li et al. 2013). The functionalized electrode was suspended in AHAb solution overnight at 4 ºC under static condition and rinsed with PBS to remove non-specific adsorption. The biosensor was incubated in 5% (m/v) BSA solution at 37 ºC under 5% $CO_2$ and 95% air for 5 min to block the activated carboxyl groups that are not coated with the amino groups of AHAb. The electrode was rinsed with PBS for three times. The anti- HER2 antibody was finally immobilized on the functionalized electrode to enable the detection of $HER2^+$ cancer cells.

*2-4 Cell culture and detection of cancer cells*

The breast cancer cell line SK-BR3 ($HER2^+$ cancer cells with the expression level of 3), breast cancer cell line ZR-75-1 ($HER2^+$ cancer cells with the expression level of 2), MDA-MB231 ($HER2^-$ cancer cells with the expression level of 0-1), colon cancer cell line SW742 and normal MCF10A breast cell line (with the expression level of 0-1) were cultured in DMEM (Dulbecco's Modified Eagle's Medium), 10% FBS and 1% antibiotic (penicillin-streptomycin solution), at 37 ºC in a humidified incubator (5% $CO_2$ and 95% humidity) (Benavides et al. 2009; Merlin et al. 2002; Subik et al. 2010; Wolff et al. 2007). After culturing the cells for three days, they were collected with 1% trypsin/EDTA. To detect cancer cells with the nano-biosensor, the electrodes were immersed in a defined concentration of cells in the DMEM culture medium within a cell culture incubator. After incubation for enough time, non-specific adsorbed cells were removed with 0.5% Tween-20 and rinsed with PBS. To determine electrochemically the concentration of cancer cells on the electrode, the electrical current signal of the nano-biosensor was recorded in PBS solution containing 2.5 mM $K_3Fe(CN)_6$ and 2.5 mM $K_4Fe(CN)_6$ as the redox probe. Differential pulse voltammetry (DPV)



Accepted manuscript

ACCEPTED MANUSCRIPT

method was used to measure the current in the potential range of -200 to 600 mV with the scan rate of 100 $mV.s^{-1}$ as a result of the immunological interaction of AHAb and HER2 antigens overexpressed on the cancer cells. The change of current density ($\Delta j$) against different concentrations of cancer cells was taken as the analytical signal.

## 3- RESULTS AND DISCUSSION

### *3.1 Principle of nano-biosensing of $HER2^+$ cancer cells*

The schematic presentation of the synthesis steps of the sandwich model of NFG/AgNPs/PANI nanocomposite and its biosensing application for detection of $HER2^+$ cancer cells is shown in **Fig. 1A**. The nanocomposite was constructed using a stepwise technique. First, NFG was deposited on the surface of FTO as the substrate to increase the surface area and charge transfer conductance. NFG was then decorated with AgNPs to enhance the stability of the nanocomposite and improve the adherence of the upper PANI layer. Finally, PANI was electropolymerized on the AgNPs layer to increase the sensitivity, a better interaction of the electrode with AHAb, and accomplish the pellet/flake-like structure of the three-layer nanocomposite (**Fig. 1B**).

SK-BR3 breast cancer cells that highly overexpress HER2 gene product were detected using our nano-biosensor. The FESEM images of **Fig. 1C** and **D** show the stability of the antibody and the cell captured on the electrode surface, respectively. The successful immobilization and deposition of AHAb on the electrode surface (**Fig. 1C**) changed the surface of the nanocomposite. **Fig. 1D** show a sample SK-BR3 cancer cell deposited on the antibody after incubation of $5\times10^3$ $cells.mL^{-1}$ with the probe surface. The cells were fixed with 2.5% glutaraldehyde solution for 6 h and washed with PBS for 15 min. The electrode probe was then dehydrated with alcohols and dried in air. The massive mass shown in **Fig. 1D** shows one single cancer cell captured on AHAb coated surface.

Accepted manuscript

ACCEPTED MANUSCRIPT

The cancer cells of different concentrations captured on the electrode surface were stained and counted using 4', 6-diamidino-2-phenylindole (DAPI) fluorescent labeling the cells nuclei (**Fig. S1**).

**<<Fig. 1>>**

*3.2 Electrochemical characterization of the synthesized nanocomposite and functionalized electrode*

Nyquist plots were obtained to characterize electrochemically the surface alteration of the electrode after subsequent modification of the electrode with nanocomposite, AHAb, BSA and cancer cell in $Fe(CN)_6^{3-/4-}$ probe (**Fig. 2**). The charge transfer resistance ($R_{ct}$) of the bare FTO was about 11,000 Ω which reduced significantly after deposition of the NFG/AgNPs/PANI nanocomposite on the FTO (**Fig. 2**). The drop of resistance greatly increased the sensitivity of the electrode and improved the detection limit. Binding of the antibody on the nanocomposite surface increased the $R_{ct}$ significantly because the antibody biomolecule was not electroactive and once deposited blocked the surface and inhibited the charge transfer. A subsequent incorporation of BSA to the surface also increased the $R_{ct}$. Incubation of the functionalized electrode with cancer cells led to a selective immobilization of cancer cells to the electrode and increased the $R_{ct}$ extensively because of the specific adsorption between the antibody and antigen. The non-electroactive cells block a large surface area of the electrode and prevent the electron transfer of the nanocomposite with a redox probe (Li et al. 2013).

**<<Fig. 2>>**

*3.3 Optimization of the functionalization process and sensor performance*

The difference between the electrical current of each electrode with immobilized cells respect to the electrical current detected in BSA treatment step ($\Delta j$) was selected as the criterion to evaluate the effect of every parameter on functionalization and sensing performance. The $\Delta j$ for bare FTO and FTO modified with NFG, NFG/AgNPs, PANI and NFG/PANI electrodes were measured (**Fig. 3A**)



Accepted manuscript

ACCEPTED MANUSCRIPT

and compared to $\Delta j$ of NFG/AgNPs/PANI. The results show that the nanocomposite combination of NFG, PANI and AgNPs resulted in the highest $\Delta j$ and had a favorable effect on highly sensitive detection of breast cancer cells. Moreover, among different components of this nanocomposite, the size of AgNPs showed a vital effect on the performance of nanocomposite architecture and function. NFG/AgNPs/PANI nanocomposite was synthesized under different duration of AgNPs electrodeposition (electrodeposition duration of 10 and 90, 1 and 90, and 1 and 30 s for $E_1$ and $E_2$, respectively) shown in **Fig. 3B**. The duration $E_1$ is dedicated to the deposition of AgNPs cores and the duration $E_2$ is devoted to the growth of nanoparticle cores. The results show a more appropriate number of cores formed for $E_1$ duration of 1 s. Also for $E_2$ duration of 90 s, the AgNPs cores showed a delicate growth needed for better electropolymerization of PANI and deposition of an appropriate number of antibodies on the electrode surface (Geboesa et al. 2014; Ustarroz et al. 2010). The optimal duration for the deposition and growth of AgNPs cores were set to 1 s and 90 s, respectively.

The effect of several experimental parameters such as anti-HER2 concentration, immune incubation time, temperature, and pH were also optimized to achieve a higher performance sensing. First, the electrodes were immersed in different concentrations of AHAb (10, 50, 100, 150, 200, 250, and 300 $\mu g.mL^{-1}$) and subjected to the incubation with $5\times10^4$ $cells.mL^{-1}$ SK-BR3 cancer cells. The $\Delta j$ increased with increasing the concentration of AHAb until 200 $\mu g.mL^{-1}$ (**Fig. 3C**). However, no significant change in the electrical current was observed for the AHAb concentration above 200 $\mu g.mL^{-1}$ because the electrode surface functionalized with ―COOH group were saturated with the antibody (Zhu et al. 2012). Therefore, 200 $\mu g.mL^{-1}$ concentration of AHAb was selected to be the optimal concentration. Second, to optimize the incubation time of the $HER2^+$ cancer cells and the immobilized antibody, the sensor was incubated for 5, 15, 30, 60, 120, and 180 min in $5\times10^4$ $cells.mL^{-1}$ SK-BR3 cancer cells. The $\Delta j$ value first increased with increasing the incubation time



Accepted manuscript

ACCEPTED MANUSCRIPT

and then remained almost constant after 30 min incubation due to the electrode saturation. Therefore, the optimal incubation duration was selected to be 30 min (**Fig. 3D**). Furthermore, the effect of temperature on the electrochemical cell and redox probe was investigated where the redox probe was tested at different temperatures of 19, 25, 35, 45, 55, and 65 ºC. The optimal response was observed at 35 ºC that is near to human body temperature where $\Delta j$ is maximum maybe due to a gradual denaturation of biomolecules at higher temperatures (**Fig. 3E**) (Deng et al. 2017). Finally, the effect of pH parameter was studies given the fact that the electrostatic states and configurations of proteins (here antibody) are commonly affected by media pH (**Fig. 3F**). The results show that the antibody and cells are denatured completely at low pH (acidic pH = 2), indicated by the negative value of the $\Delta j$. No significant change in the $\Delta j$ value was detected for pH values higher than the neutral pH optimal value of 7.4, indicating that proteins were not denatured for pH above 7.4. Each test of the optimization was repeated on three separate electrodes, and the results showed a high reproducibility of the electrodes.

**<<Fig. 3>>**

*3.4 Dynamic detection range, detection limit and selectivity of the nano-biosensor*

The optimized electrochemical cell and probe were used to obtain the dynamic detection range of the biosensor for detecting $HER2^+$ SK-BR3 cancer cells in $Fe(CN)_6^{3-/4-}$ and PBS solution. Differential pulse (DP) voltammograms for different concentrations of breast cancer cells are shown in **Fig. 4A**. The nano-biosensor showed a calibration curve of $R^2 = 0.9926$, n = 3, and RSD < 5%. The dynamic detection range of the biosensor was determined to be $10 - 5\times10^6$ cells.mL$^{-1}$, much superior than other labeled and label-free sensors used for cancer cell detection. Applying S/N = 3 criterion, the sensor demonstrated a detection limit of 2 cells.mL$^{-1}$ (**Fig. 4B**) which had an excellent performance in compared to other cancer cell detecting sensors (**Table 1**). The logarithmic function of cell concentration was used to achieve a linear function for $\Delta j$ with respect



Accepted manuscript

ACCEPTED MANUSCRIPT

to the concentration of cells, (Log [cell]). The rationale behind this success is resulted from the design and synthesis of a sandwich architecture and ultrapure nanocomposite with a high conductivity and charge transfer, necessary for the detection of non-electroactive materials like biomolecules and cells. The repeatability of the biosensor was further examined where $\Delta j$ was determined to be 49.716 ± 2.227 (n = 3, RSD = 4.5%) for $5\times10^4$ cells. $mL^{-1}$ SK-BR3 cancer cells, indicating a strong binding of SK-BR3 cells to antibodies through specific immunoreaction. To evaluate the stability of the biosensor, the functionalized electrode was stored at 4 ºC for 15, 30, and 45 days and tested for the detection of SK-BR3 cancer cells. The results showed that the biosensor preserved its detection efficiency for about 99.9% and remained very stable even after 45 days storage (**Fig. S2**).

**<<Fig. 4>>**

**<<Table. 1>>**

To assess the selectivity of the nano-biosensor for the detection of HER2-expressing SK-BR3 cancer cells, other types of cells, including breast cancer cell line ZR-75-1 ($HER2^+$ cancer cells with the middle expression level), colon cancer cell line SW742, breast cancer cell line MDA-MB231 (without or with low expression level of HER2), and normal MCF10A breast cell line were examined.

The results show a significance decrease in the $R_{ct}$ and as a consequence a negative value of the $\Delta j$ for the last three types of cells. The negative $\Delta j$ is mainly because of the very weak binding between these $HER2^-$ cancer cells and the HER2 functionalized electrode, where the cells were detached when they were subjected to Tween-20 washing. Moreover, washing the electrode not only removed the $HER2^-$ or weak HER2-expressing cancer cells but also the BSA proteins, which resulted in a high value of RSD for $HER2^-$ cancer cells.

Accepted manuscript

ACCEPTED MANUSCRIPT

Clinically, the number of HER2 overexpressed cancer cells in 1 mL blood represents the level of breast cancer and can be used to determine the efficacy of therapeutics. The nano-biosensors developed in this work is highly specific to HER2 antigen where the interaction between the antibody and HER2 antigen is strong enough to withstand the washing forces, which only happens for cancer cells with overexpressed or middle expressed HER2. This could distinguish between the targeted cells (HER2 positive cancer cells) and the cells with low expressed HER2. The detection of medium HER2 expressed ZR-75-1 breast cancer cells, in particular, was tested to evaluate the sensitivity of the nano-biosensor to the level of HER2 expression (Subik et al. 2010). The nano-biosensor successfully distinguished between SK-BR3 and ZR-75-1 where the intensity of current peak for ZR-75-1 was approximately one-third of the intensity of current peak for SK-BR3 for the same concentration of cells (**Fig. 5A**). The expression level of HER2 significantly affects the level of interaction between anti-HER2 and cancer cells, which makes the nano-biosensor not only selective to HER2 positive cancer cells but also sensitive to their HER2 expression level.

Due to a strong immunoreaction between $HER2^+$ SK-BR3 cancer cells and anti-HER2 antibody, the interference from other $HER2^-$ cancer cells was minimal. Moreover, the specificity of the nano-biosensor was examined by testing the sensor for the detection of SK-BR3 cancer cells spiked in whole blood samples. The biosensor was immersed and incubated in $5\times10^2$, $5\times10^3$, and $5\times10^4$ SK-BR3 cancer cells spiked in 1 mL blood (3 electrodes for each cell concentration) without any preparation (heparin was added to the blood to prevent blood clotting). The recovery of the number cancer cells in blood respect to the number of cells in culture medium was reported to be 91.1, 98.9, and 96.1 %, respectively (**Fig. 5B**). There was no significant difference for the detection of different concentrations of cancer cells within culture medium and blood media ($p$ value $\leq 0.10$) (**Fig. 5C**). This indicates that the nano-biosensor developed in this work demonstrated a high functional and commercialization capabilities for the detection of breast cancer cells in clinical samples.

Accepted manuscript

ACCEPTED MANUSCRIPT

**<<Fig. 5>>**

From clinical point of view, it is worth mentioning that the calibration curve of the biosensor may be to some extent dependent upon the type of cancer cells and limit of HER2 expression level. The calibration curve for each type of cancer cells with a known HER2 expression level needs to be established by correlating the electrical signals recorded by the biosensor and the number of cells captured on the electrodes. These biosensors can be used for the diagnosis of cancer patients with a known HER2 expression level. Upon determining the initial cancer type and their level of HER2 expression using standard phase contrast microscopy, cell staining and counting, the biosensors with the calibration curve defined for a certain cancer cell type is selected to assess the efficacy of therapeutics in the course of treatment without any need to cell staining or cell counting. Further clinical implementation of these biosensors requires statistical analysis for evaluating the performance of biosensors in determining the dependency of the sensing to HER2 expression level.

Accepted manuscript

## 4- CONCLUSION

The successful implementation of NFG/AgNPs/PANI configuration as a suitable template for label-free electrochemical detection of $HER2^{+}$ cancer cells was introduced. The nano-biosensor demonstrated a highly sensitive and selective performance and detected $HER2^{+}$ SK-BR3 cancer cells with the detection limit of 2 $cells.ml^{-1}$. The biosensor also differentiated between the high HER2 expression level SK-BR3 and medium HER2 expression level ZR-75-1. This probe indicated a high selectivity in discriminating SK-BR3 cells, high stability, wide linear detection range and very low detection limit with desirable reproducibility. This nanocomposite can be functionalized with other cancer biomarkers to diagnose different stages of cancer or even other diseases. Given its simple functionalization, affordable, sensitive and robust performance biosensor with the fast

ACCEPTED MANUSCRIPT

response, one can use this sensor not only for early cancer detection but also for monitoring the efficacy of cancer therapeutics.

## REFERENCES

Ali, M.A., Mondal, K., Jiao, Y., Oren, S., Xu, Z., Sharma, A., Dong, L., 2016. ACS Applied Materials & interfaces 8(32), 20570-20582.
Benavides, L.C., Gates, J.D., Carmichael, M.G., Patel, R., Holmes, J.P., Hueman, M.T., Mittendorf, E.A., Craig, D., Stojadinovic, A., Ponniah, S., 2009. Clinical Cancer Research 15(8), 2895-2904.
Capobianco, J.A., Shih, W.Y., Yuan, Q.-A., Adams, G.P., Shih, W.-H., 2008. Review of Scientific Instruments 79(7), 076101.
Cernat, A., Tertiș , M., Păpară, C.N., Bodoki, E., Săndulescu, R., 2015. Int. J. Electrochem. Sci 10, 4718-4731.
Chan, D.W., Beveridge, R.A., Bhargava, A., Wilcox, P.M., Kennedy, M.J., Schwartz, M.K., 1994. American Journal of Clinical Pathology 101(4), 465-470.
Cho, H.-S., Mason, K., Ramyar, K.X., Stanley, A.M., 2003. Nature 421(6924), 756-760.
Chung, J., Bernhardt, R., Pyun, J., 2006. Sensors and Actuators B: Chemical 118(1), 28-32.
Darowicki, K., Kawula, J., 2004. Electrochimica Acta 49(27), 4829-4839.
De la Escosura-Muñiz, A., Sánchez-Espinel, C., Díaz-Freitas, B.n., González-Fernández, A.f., Maltez-da Costa, M., Merkoc□i, A., 2009. Analytical Chemistry 81(24), 10268-10274.
Deng, H., Liu, Q., Wang, X., Huang, R., Liu, H., Lin, Q., Zhou, X., Xing, D., 2017. Biosensors and Bioelectronics 87, 931-940.
Ding, L., Ji, Q., Qian, R., Cheng, W., Ju, H., 2010. Analytical Chemistry 82(4), 1292-1298.
Feng, L., Chen, Y., Ren, J., Qu, X., 2011. Biomaterials 32(11), 2930-2937.
Galletti, G., Sung, M.S., Vahdat, L.T., Shah, M.A., Santana, S.M., Altavilla, G., Kirby, B.J., Giannakakou, P., 2014. Lab on a Chip 14(1), 147-156.
Gao, J., Chen, K., Miao, Z., Ren, G., Chen, X., Gambhir, S.S., Cheng, Z., 2011. Biomaterials 32(8), 2141-2148.
Geboesa, B., Vanrenterghema, B., Ustarrozb, J., Pauwelsa, D., Sotiropoulosc, S., Hubinb, A., Breugelmansa, T., 2014. Chemical Engineering 41, 73-78.
Gown, A.M., 2008. Modern Pathology 21(S2), S8-S15.
Gruhl, F.J., Rapp, M., Länge, K., 2010. Procedia Engineering 5, 914-917.
Gullick, W.J., 2001. Breast Cancer Research 3(6), 390-394.
Han, Q., Wang, R., Xing, B., Chi, H., Wu, D., Wei, Q., 2018a. Biosensors and Bioelectronics 106, 7-13.
Han, Q., Wang, R., Xing, B., Zhang, T., Khan, M.S., Wu, D., Wei, Q., 2018b. Biosensors and Bioelectronics 99, 493-499.
Hathaway, H.J., Butler, K.S., Adolphi, N.L., Lovato, D.M., Belfon, R., Fegan, D., Monson, T.C., Trujillo, J.E., Tessier, T.E., Bryant, H.C., 2011. Breast Cancer Research 13(5), R108.
Jiang, K., Almhanna, K., Henderson-Jackson, E., Malafa, M., Coppola, D., 2014. American Journal of Clinical Pathology 142(suppl_1), A176.
Kearney, A.J., Murray, M., 2009. Journal of Midwifery & Women's Health 54(5), 393-400.
Khoo, B.L., Grenci, G., Lim, Y.B., Lee, S.C., Han, J., Lim, C.T., 2018. nature protocols 13(1), 34-58.
Li, H., He, J., Li, S., Turner, A.P., 2013. Biosensors and Bioelectronics 43, 25-29.



Accepted manuscript

ACCEPTED MANUSCRIPT

Li, K., Zhan, R., Feng, S.-S., Liu, B., 2011. Analytical Chemistry 83(6), 2125-2132.
Li, T., Fan, Q., Liu, T., Zhu, X., Zhao, J., Li, G., 2010. Biosensors and Bioelectronics 25(12), 2686-2689.
Lu, W., Arumugam, S.R., Senapati, D., Singh, A.K., Arbneshi, T., Khan, S.A., Yu, H., Ray, P.C., 2010. ACS Nano 4(3), 1739-1749.
Mass, R.D., Press, M.F., Anderson, S., Cobleigh, M.A., Vogel, C.L., Dybdal, N., Leiberman, G., Slamon, D.J., 2005. Clinical Breast Cancer 6(3), 240-246.
Mayer, J.A., Pham, T., Wong, K.L., Scoggin, J., Sales, E.V., Clarin, T., Pircher, T.J., Mikolajczyk, S.D., Cotter, P.D., Bischoff, F.Z., 2011. Cancer Genetics 204(11), 589-595.
Merlin, J.-L., Barberi-Heyob, M., Bachmann, N., 2002. Annals of Oncology 13(11), 1743-1748.
Myung, S., Solanki, A., Kim, C., Park, J., Kim, K.S., Lee, K.B., 2011. Advanced Materials 23(19), 2221-2225.
Ohno, Y., Maehashi, K., Matsumoto, K., 2010. Journal of the American Chemical Society 132(51), 18012-18013.
Reátegui, E., Aceto, N., Lim, E.J., Sullivan, J.P., Jensen, A.E., Zeinali, M., Martel, J.M., Aranyosi, A.J., Li, W., Castleberry, S., 2015. Advanced Materials 27(9), 1593-1599.
Riccio, G., Esposito, G., Leoncini, E., Contu, R., Condorelli, G., Chiariello, M., Laccetti, P., Hrelia, S., D'Alessio, G., De Lorenzo, C., 2009. The FASEB Journal 23(9), 3171-3178.
Salahandish, R., Ghaffarinejad, A., Naghib, S.M., Majidzadeh-A, K., Sanati-Nezhad, A., 2018. IEEE Sensors Journal 18(6), 2513-2519.
Sieben, V., Marun, C.D., Pilarski, P., Kaigala, G., Pilarski, L., Backhouse, C., 2007. Iet Nanobiotechnology 1(3), 27-35.
Slamon, D., Clark, G., Wong, S., Levin, W., Ullrich, A., McGuire, W., 1987. Science 235(4785), 177-182.
Subik, K., Lee, J.-F., Baxter, L., Strzepek, T., Costello, D., Crowley, P., Xing, L., Hung, M.-C., Bonfiglio, T., Hicks, D.G., 2010. Breast Cancer: Basic and Clinical Research 4, 35-41.
Tsai, M.-C., Tsai, T.-L., Shieh, D.-B., Chiu, H.-T., Lee, C.-Y., 2009. Analytical hemistry 81(18), 7590-7596.
Ustarroz, J., Gupta, U., Hubin, A., Bals, S., Terryn, H., 2010. Electrochemistry Communications 12(12), 1706-1709.
Vaisocherová, H., Faca, V.M., Taylor, A.D., Hanash, S., Jiang, S., 2009. Biosensors and Bioelectronics 24(7), 2143-2148.
Wang, X., Xu, R., Sun, X., Wang, Y., Ren, X., Du, B., Wu, D., Wei, Q., 2017. Biosensors and Bioelectronics 96, 239-245.
Wang, X., Zhao, M., Nolte, D.D., 2009. Analytical and Bioanalytical Chemistry 393(4), 1151.
Washburn, A.L., Gunn, L.C., Bailey, R.C., 2009. Analytical Chemistry 81(22), 9499-9506.
White, I.M., Oveys, H., Fan, X., 2006. Optics etters 31(9), 1319-1321.
Winham, S.J., Mehner, C., Heinzen, E.P., Broderick, B.T., Stallings-Mann, M., Nassar, A., Vierkant, R.A., Hoskin, T.L., Frank, R.D., Wang, C., 2017. Breast Cancer Research and Treatment 166(2), 641-650.
Wolff, A.C., Hammond, M.E.H., Schwartz, J.N., Hagerty, K.L., Allred, D.C., Cote, R.J., Dowsett, M., Fitzgibbons, P.L., Hanna, W.M., Langer, A., 2007. Archives of Pathology & Laboratory Medicine 131(1), 18-43.
Zhu, X., Yang, J., Liu, M., Wu, Y., Shen, Z., Li, G., 2013. Analytica Chimica cta 764, 59-63.
Zhu, Y., Chandra, P., Shim, Y.-B., 2012. Analytical Chemistry 85(2), 1058-1064.

Accepted manuscript

ACCEPTED MANUSCRIPT

## ASSOCIATED CONTENT

### Supporting Information

Fluorescent microscopy images of stained cancer cells and electrochemical investigation of the nano-biosensor stability.

## AUTHOR INFORMATION

Accepted manuscript

## Acknowledgments

We gratefully acknowledge the support of this work by Research Councils of Iran University of Science and Technology (IUST), Breast Cancer Research Center (BCRC), University of Calgary's

ACCEPTED MANUSCRIPT

Early Cancer Detection Initiative Fund, the CMC Canadian Microsystem, and the Natural Sciences and Engineering Research Council of Canada (NSERC). We thank Dr. Don Morris for his support in providing ZR-75-1 breast cancer cell line.

**Notes**

The authors declare no competing financial interests.

Accepted manuscript

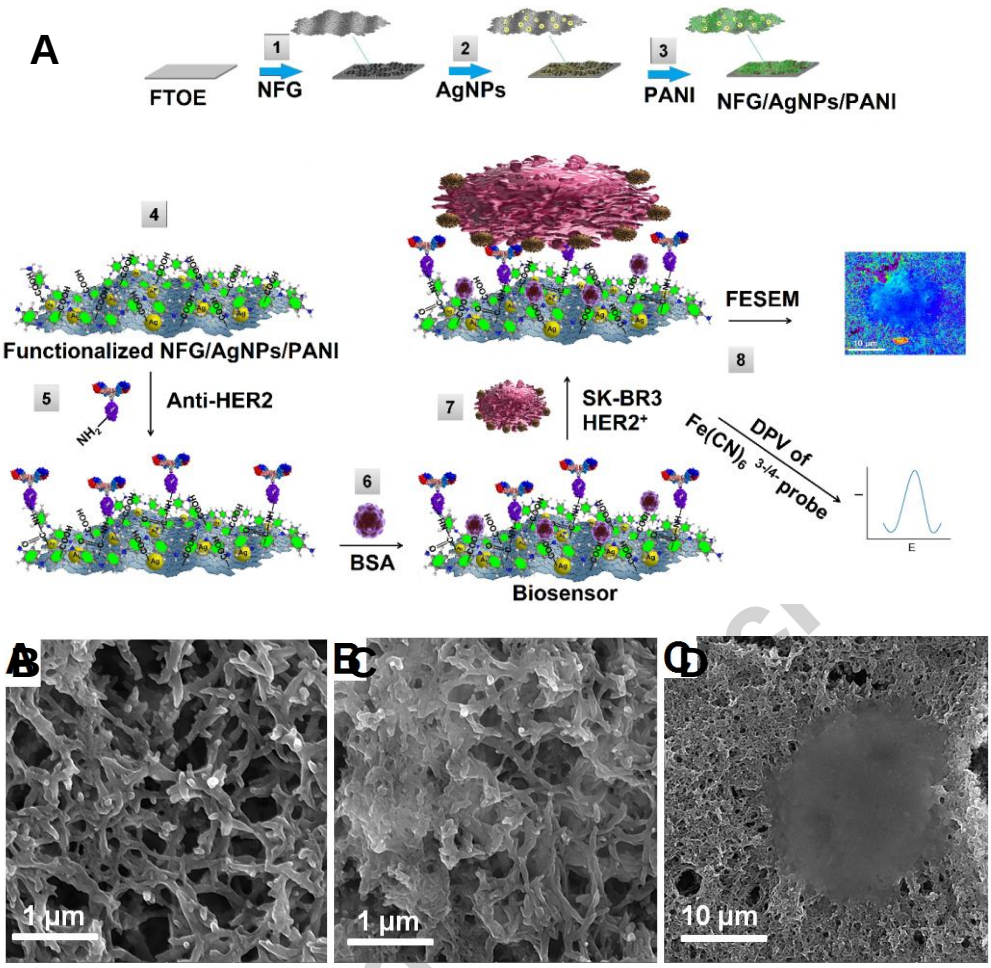


**Figure 1**. The functionalized nitrogen-doped graphene (NFG)/silver nanoparticles (AgNPs)/polyaniline (PANI) nanocomposite, functionalized electrode, and detected cancer cells over the electrode. (A) The schematic presentation of the synthesis process of NFG/AgNPs/PANI nanocomposites on the fluorine doped tin oxide (FTO) electrode in an electrochemical cell. Steps for synthesis of the nanocomposite include 1) cast coating of the NFG on the FTO electrode; 2) chronoamperometry of AgNPs on the modified FTO electrode, and 3) electropolymerization of aniline monomers on the modified FTO electrode by cyclic voltammetry (CV) cycles. The schematic of the experimental setup is shown at the top. The schematic image at the bottom represents the fabrication steps of the diagnostic biosensor of SK-BR3 breast cancer cells over the FTO electrode; 4) a summary of the protocol used for functionalizing the nanocomposite; 5) immobilization of the antibody; 6) blocking the surface with bovine serum albumin (BSA); 7) immersing the biosensor in culture medium with spiked breast cancer cells; and 8) detection of SK-BR3 by FESEM and electrochemical method (Differential pulse voltammetry (DPV)). (B), (C), and (D) The FESEM micrographs of the nanocomposite (NFG/AgNPs/PANI), nanocamposite/anti-HER2 antibody (AHAb), and nanocamposite/AHAb/SK-BR3 cancer cells, respectively.

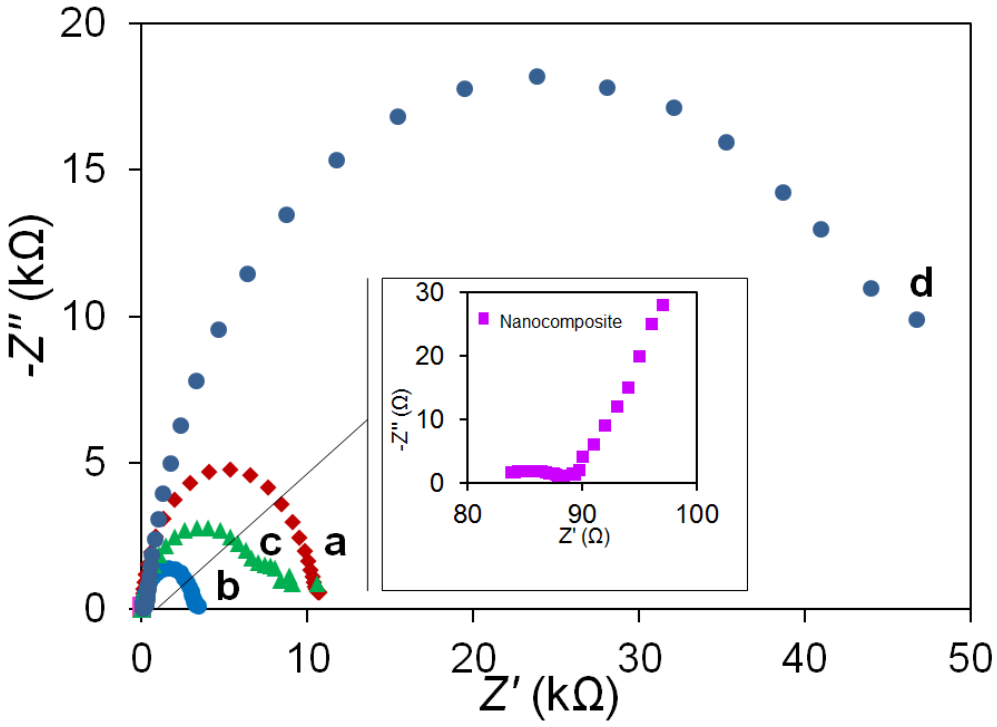


**Figure 2.** Nyquist plots of a) FTO, b) nanocomposite/AHAb, c) nanocomposite/AHAb/BSA, and d) nanocomposite/AHAb/BSA/SK-BR3 breast cancer cells for characterizing the surface alteration of electrode after subsequent modification in 2.5 mM $K_3Fe(CN)_6$ + 2.5 mM $K_4Fe(CN)_6$ and 0.02 M PBS (Inset is the Nyquist plot for the nanocomposite of NFG/AgNPs/PANI).

Accepted manu

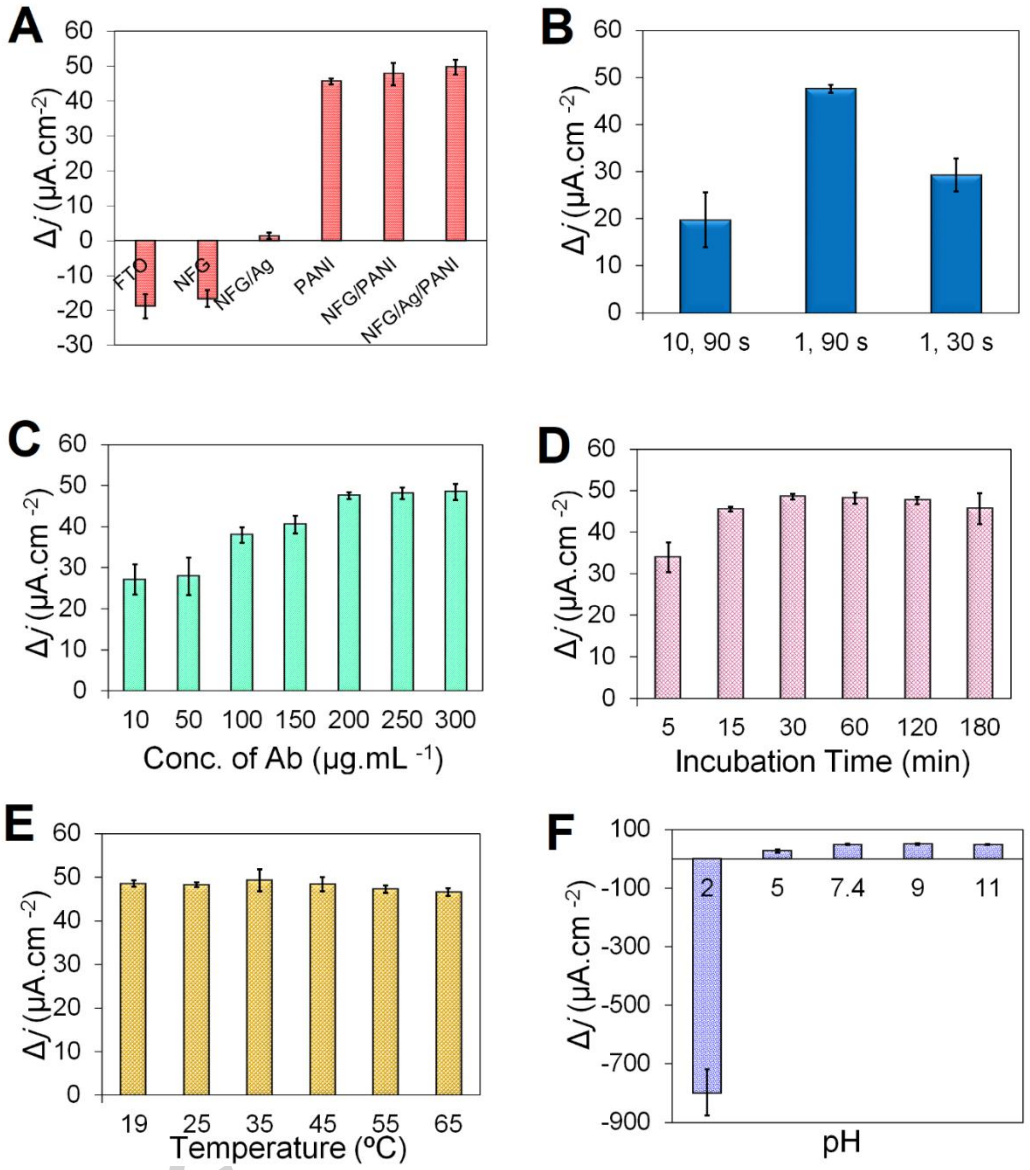


**Figure 3.** Optimization of the electrode functionalization protocol. (A) The effect of different coating over the FTO electrode on sensitivity of cancer cell detection. (B) The effect of AgNPs size on the sensitivity of cancer cell detection. The duration of electrodeposition are 10 s and 90 s, 1 s and 90 s, and 1 s and 30 s for $E_1$ and $E_2$, respectively. The effect of (C) AHAb concentration, (D) incubation time, (E) temperature of testing in the presence of redox probe, and (F) pH of the solution on efficiency of the biosensor (NFG/AgNPs/PANI modified electrode). The tests were done in a solution containing 2.5 mM $K_3Fe(CN)_6$ + 2.5 mM $K_4Fe(CN)_6$ and 0.02 M PBS. Every measurement was repeated three times by three different probes.

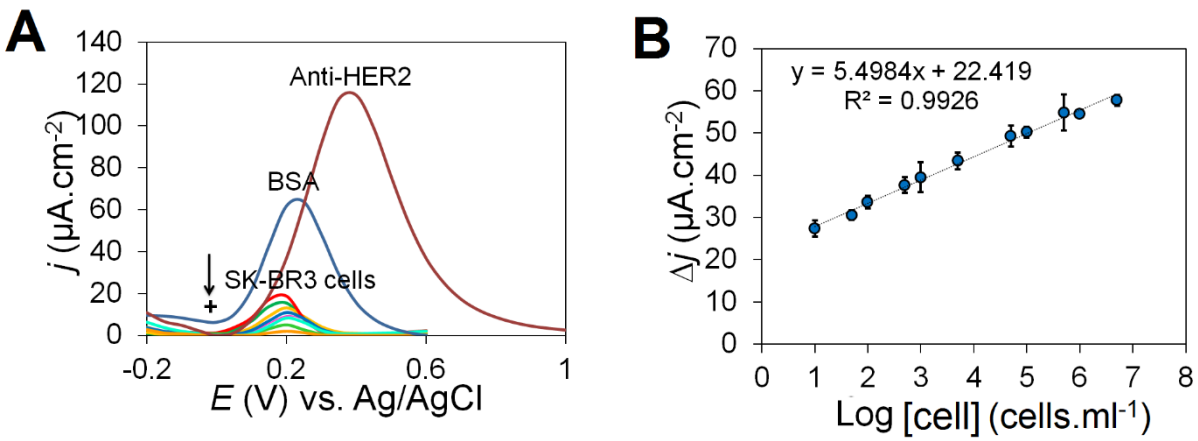


**Figure 4.** Detection of cancer cells. (A) Differential pulse (DP) voltammograms at 100 $mV.s^{-1}$ scan rate for AHAb, BSA and different concentrations of breast cancer cells, and (B) calibration curve for different concentrations of SK-BR3 breast cancer cells under optimal sensing conditions. These tests were performed in a solution containing 2.5 mM $K_3Fe(CN)_6$ + 2.5 mM $K_4Fe(CN)_6$ and 0.02 M PBS. Every measurement was repeated three times by three different probes.

Accepted manuscript

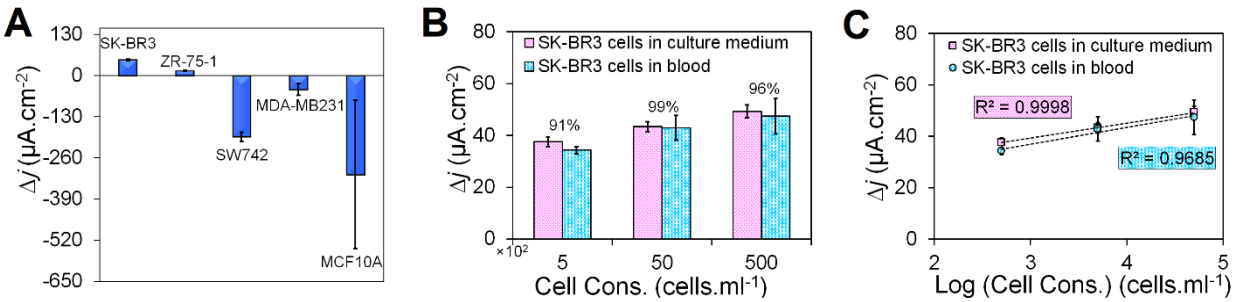


**Figure 5.** Nano-biosensing of cancer cells expressing different levels of HER2. (A) The selectivity of the sensor in the presence of $5\times10^4$ cells.mL$^{-1}$ ZR-75-1 breast cancer cells (HER2$^+$ middle expression level), SW742 colon cancer cells, MDA-MB231 breast cancer cells (expression level 0-1), and normal MCF10A breast cells, individually. The SK-BR3 concentration is the same as the concentration of other cell types. These tests were performed in a solution containing 2.5 mM $K_3Fe(CN)_6$ + 2.5 mM $K_4Fe(CN)_6$ and 0.02 M PBS. Every measurement was repeated three times by three different probes. (B) Recoveries and (C) Calibration curves obtained for the detection of SK-BR3 breast cancer cells in the blood samples and culture medium. The concentrations of cancer cells were set to be $5\times10^2$, $5\times10^3$, and $5\times10^4$ cells.mL$^{-1}$.

Accepted manuscript

ACCEPTED MANUSCRIPT

**Table 1.** Performance comparison of our nano-biosensor coated with NFG/AgNPs/PANI nanocomposites respect to the biosensors developed previously.

| Cell type | Material | Detection technique | Dynamic range (cells. $mL^{-1}$) | Detection limit (cells. $mL^{-1}$) | Reference |
|---|---|---|---|---|---|
| Cervical cancer (Hela) | Graphene | Label-free electrochemical sensor | $1\times10^3 - 1\times10^6$ | 794 | (Feng et al. 2011) |
| Breast cancer (SK-BR3) | Oval shaped AuNP | Colorimetric/two photon scattering | - | 100 | (Lu et al. 2010) |
| Breast cancer (SK-BR3) | Hydrazine−Au Nanoparticle−Aptamer | Labeled electrochemical sensor | $50 - 2\times10^4$ | 26 | (Zhu et al. 2012) |
| Breast cancer (MCF7) | Au electrode/Aptamer | Labeled electrochemical sensor | $1\times10^4 - 1\times10^7$ | 3300 | (Li et al. 2010) |
| Dynamic Carbohydrate Expression on Living Cells | Carbon nanohorns | Electrochemical sensor | $2\times10^3 - 2\times10^6$ | 1500 | (Ding et al. 2010) |
| Blood cancer | AuNPs | Electrochemical sensor | $8\times10^3 - 4\times10^5$ | 4000 | (de la Escosura-Muñiz et al. 2009) |
| Breast cancer (MCF7) | Au electrode/Aptamer | Labeled electrochemical sensor | $1\times10^2 - 1\times10^7$ | 100 | (Zhu et al. 2013) |
| **Breast cancer (SK-BR3)** | **NFG/AgNPs/PANI** | **Label-free electrochemical sensor** | **$10 - 5\times10^6$** | **2** | **Present work** |

Accepted manuscript

ACCEPTED MANUSCRIPT

## Highlights;

- Highly sensitive and selective electrochemical biosensor for detecting HER2 biomarker
- Distinguishing cells with various levels of HER2 expression
- Ability to detection of single cancer cell with significant repeatability
- Extremely low response time with respect to other biosensors

Accepted manuscript